

# Oscillations and defect turbulence in a shallow fluidized bed

D.K.Clark<sup>1</sup>, L.S. Tsimring<sup>1</sup>, and I.S.Aranson<sup>2</sup>

<sup>1</sup>*Institute for Nonlinear Science, University of California, San Diego, La Jolla, CA 92093-0402*

<sup>2</sup>*Materials Science Division, Argonne National Laboratory, Argonne, IL 60439*

(February 8, 2008)

We report an experimental study of the dynamics of an air-fluidized thin granular layer. Near-onset behavior of this shallow fluidized bed was described in the earlier paper (Tsimring et al, 1999). Above the threshold of fluidization the system exhibits a Hopf bifurcation as the layer starts to oscillate at a certain frequency due to a feedback between the layer dilation and the airflow drag force. After application of temporal band-pass filtering of this frequency we discovered the spatio-temporal dynamics in the form of defect turbulence. This type of dynamics is natural for spatio-temporal systems close to the threshold of a Hopf bifurcation. At high flow rates, low-frequency short-wavelength structures appear in addition to the long-wavelength excitations. A simple model describing the instability and occurrence of oscillations in a shallow fluidized bed, is proposed.

PACS: 46.10.+z, 47.54.+r, 47.35.+i

The non-equilibrium dynamics of granular materials have been a subject of growing attention among physicists in the last few years [1–3]. Granular materials reveal a host of interesting phenomena (compaction, self-organized criticality, patterns, convection, etc.) when are subjected to external driving. A typical way of driving the granular medium out of equilibrium is to fluidize it with an external gas or liquid flow. Such “fluidized beds” are widely used in the industry for mixing solid and liquid chemicals [4,5]. One of the biggest problems associated with this use of fluidized beds is an instability which leads to macroscopic inhomogeneities and fluctuations in the bulk (bubbling, slugging). At large flow rates, this leads to a developed three-dimensional turbulent regime resembling boiling liquid.

In the recent paper [6], we proposed to study the dynamics of air-fluidized granular materials in a bed with a large aspect ratio between the horizontal size and the thickness of the layer. In this geometry, the dynamics become quasi-two-dimensional and can be investigated by imaging the surface of the granular layer. In Ref. [6], we studied the onset of fluidization and found that it has the features of a phase transition, with very long transient fluctuations just below the fluidization threshold. In this paper, we report the results of the experimental study of the thin granular layer dynamics at high airflow rates, above the threshold of fluidization. We find that above this threshold the layer begins to oscillate at a certain frequency which depends on the layer thickness and the airflow rate. Processing of surface images revealed the occurrence of propagating waves which form small disordered short-lived spirals. At larger airflow rate, irregular small-scale oscillating cellular pattern appears on the surface of the bed. The temporal frequency of these oscillating bubbles is significantly less than that of large-scale waves. We believe that these small-scale perturbations are generated by the large amplitude, long-wave

layer oscillations in a way similar to the mechanism of Faraday instability in fluid or granular layers subject to external vertical vibrations (see, e.g., [2,7]). The mechanism of layer oscillations is related to the dependence of the drag force from the air flow acting on the granular layer, on the volume fraction of particles in the layer. When the layer is dilated, the drag force diminishes, and the layer falls back due to gravity. This picture leads us to the formulation of the simple dynamical model which qualitatively agrees with our experimental results.

The experimental setup is similar to the one used in Ref. [6], but it features a larger round porous bronze plate (diameter 15 cm, thickness 0.5 cm, average pore size  $6\mu\text{m}$ ). As a fluidizing fluid we use compressed dry air. The granular material consists of monodisperse spherical bronze particles of size 0.15 mm, and the bed depth was varied from 3 to 7 particles deep. The patterns on the surface of the granular layer were illuminated using the low-angle light from a circular fluorescent light around the bed, and recorded using high-speed Kodak SR-C digital CCD camera. We also used a pressure transducer SenSym SX01DP1 to record the airflow fluctuations near the free surface of the granular layer.

When the flow rate is below certain threshold value, the layer remains completely static. The value of this critical airflow depends sensitively on the grain parameters (size, shape, density) as well as on the thickness of the layer. Unless explicitly noted otherwise, we will be referring to the bed thickness 0.65 mm. For that thickness, the critical airflow speed was 12.1 cm/sec. Slightly above the threshold, the fluidization of the layer is highly non-uniform. As described in our earlier paper Ref. [6], the fluidization occurs in small localized regions surrounded by completely static grains.

At higher values of the airflow the whole layer becomes fluidized and exhibits noticeable vertical oscillations. The power spectrum of the pressure fluctuations near the

free surface of the layer is shown in Figure 1. We measured the peak frequency and the magnitude as a function of the airflow velocity (Figure 2). The amplitude of the oscillations increases linearly and the frequency  $f$  slightly decreases as the airflow speed increases. Figure 3a shows dependence of the peak frequency on the airflow speed for different values of layer thickness. A naive scaling of variables by the gravity  $g$  and the thickness of the layer  $h_0$  ( $f(h_0/g)^{1/2}$ ,  $V(gh_0)^{-1/2}$ ) does not converge these data to a single curve. It indicates that additional non-dimensional parameters involving the particle size  $d$  and the air viscosity  $\nu$  play an important role in the mechanism of these oscillations. For example, if one chooses scaling  $Vd/(h_0^3g)^{1/2}$  for the airflow, then the data lie rather close to a single curve (see Fig.3b).

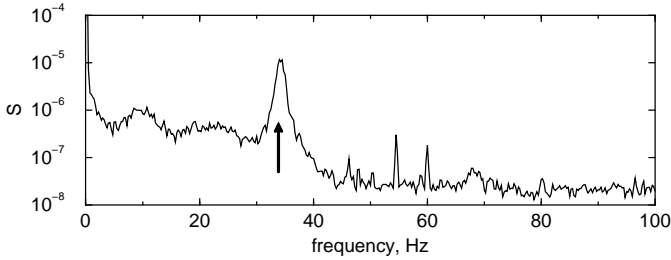


FIG. 1. Power spectrum of the pressure fluctuations near the layer at the airflow rate 15.8 cm/sec. The arrow indicates the peak corresponding to the large-scale layer oscillations.

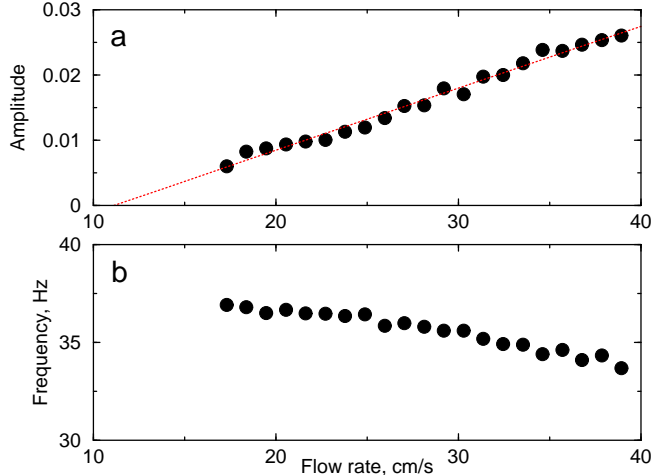


FIG. 2. Amplitude (a) and frequency (b) of the spectral peak in the power spectrum of layer oscillations as a function of the airflow rate  $V$  for the layer thickness 0.65 mm. Linear regression of the amplitude (dashed line in a) yields the oscillation threshold of 11.2 cm/s, which is slightly lower than the fluidization threshold 12.1 cm/s

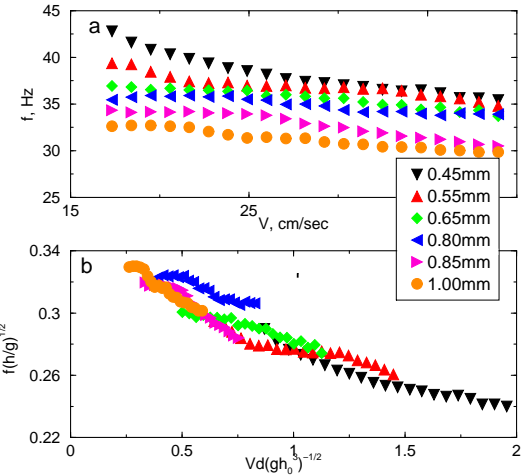


FIG. 3. a - frequency  $f$  of the spectral peak in the power spectrum of layer oscillations as a function of the airflow rate  $V$ ; b - rescaled frequency  $f(h/g)^{1/2}$  as a function of  $Vd/(gh_0)^{1/2}$

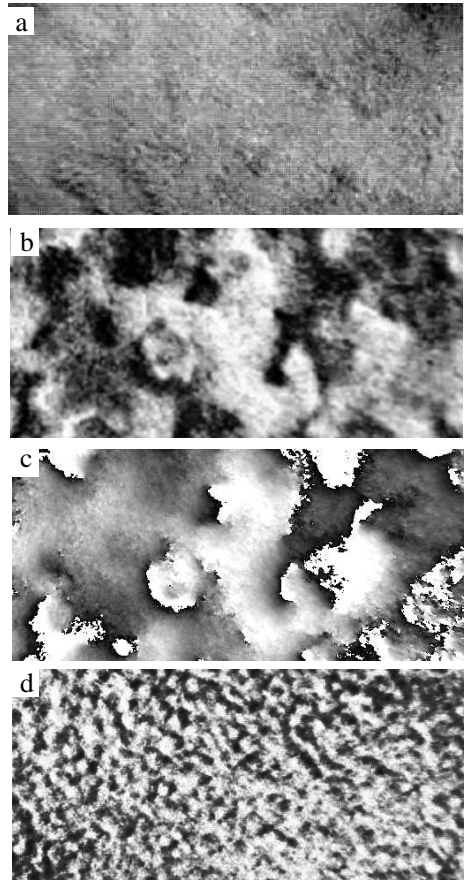


FIG. 4. Spatial structure of the 0.65 mm layer oscillations: a - snapshot of the granular layer surface for  $V = 15.8$  cm/sec; b - corresponding snapshot from the temporal sequence filtered by the narrow-band filter with central frequency  $f = 35$  Hz; c - spatial distribution of the phase of 35 Hz oscillations; d - snapshot from the temporal sequence for  $V = 42.2$  cm/sec filtered by a low-pass filter with the cutoff frequency 25 Hz.

High-speed imaging of the surface at 500 fps also confirms the occurrence of the layer oscillations. In order to determine the spatial structure of these oscillations, we performed temporal filtering of the recorded image sequences. We used a band-pass filter to extract oscillations at the peak frequency  $f$  for each pixel, and then combined these filtered signals back to create the sequence of temporally-filtered images [8].

A raw snapshot from the video sequence taken at the airflow speed 15.8 cm/sec, and the corresponding filtered snapshot are shown in Figure 4a,b. Viewing filtered images in sequence [9] reveals that the oscillations form propagating waves, moreover, these waves are organized in small irregular spirals. The sense of direction of the wave propagation can be determined from the spatial distribution of the phase of oscillations at the filtered frequency  $f$  (Figure 4c). Singularities of the phase correspond to the cores of the spirals, or topological defects. The phase distribution changes over time, as the defects move, annihilate, and new defects are born. Such “defect turbulence” is to be expected near the onset of the Hopf bifurcation in spatially extended systems. It is generically described by the Ginzburg-Landau equation for the complex amplitude of the oscillation [10]. Similar defect turbulence has been observed in spatially-extended Belousov-Zhabotinsky reaction [11].

At higher air flow, in addition to large-scale layer oscillations, irregular small-scale perturbations of the layer appear. These perturbations correspond to the low-frequency part of the layer oscillations spectrum. Figure 4d shows the snapshot of the surface image at the airflow 42.2 cm/sec obtained by low-pass filtering of the image sequence with the cut-off frequency 25 Hz. The spatial power spectrum of these perturbations averaged over angle is shown in Figure 5 together with the corresponding spectrum for the peak frequency 31 Hz. As one can see, spatial spectrum of low-frequency oscillations exhibit a broad peak at wavenumber  $k \approx 1.6 \text{ cm}^{-1}$ , whereas the spectrum of 31 Hz oscillations decays with the wavenumber.

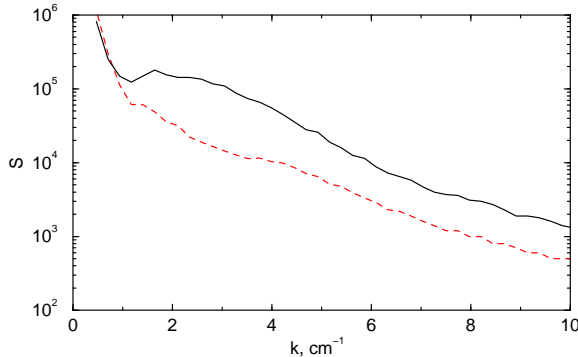


FIG. 5. Azimuthally-averaged spatial power spectrum of oscillations at the dominant frequency 31.2 Hz (dashed line) and low-frequency oscillations  $f < 25 \text{ Hz}$  (solid line) for the airflow speed 42.2 cm/sec

The mechanism of the shallow fluidized bed oscillations can be described as follows. The layer dynamics are determined by the interplay of two forces: gravity and the drag force from the gas flow. While gravity  $g$  remains constant, the drag force varies depending on the volume fraction of particles in the layer. When the layer lies on the surface and is densely packed, the drag force is maximal. On the other hand, when the layer is lifted in the air and diluted, it becomes more “transparent” for the airflow, and the drag force decreases. This effect is known for deep fluidized beds [12]. In the simplest form, we could assume that the drag force  $\Gamma$  is inversely proportional to the height of the layer  $h$ ,  $\Gamma = \gamma/h$ , where constant  $\gamma$  depends on the nominal flow speed  $V$ , close-packed thickness of the layer  $h_0$ , gas viscosity, and the properties of the individual particles (size, shape). Then the second Newton’s law yields

$$h_{tt} = \frac{\gamma}{\rho h} - g, \quad (1)$$

where subscript  $t$  denotes time derivative, and  $\rho$  is the total mass of grains per unit area. In non-dimensional variables  $H = h/h_0$  and  $T = (g/h_0)^{1/2}t$ , this equation reads

$$H_{TT} = \frac{P}{H} - 1, \quad (2)$$

where  $P = \gamma/\rho g h_0$ . The amplitude and frequency of periodic oscillations for this nonlinear oscillator equation depend on the initial conditions. Assuming that the layer always comes down to the surface where it has a minimal thickness  $h_0$ , we impose initial conditions  $H(0) = 1$  and  $H_T(0) = 0$ . With these initial conditions, amplitude  $A$  and frequency  $\Omega = \omega(h_0/g)^{1/2}$  of oscillations are uniquely determined by the parameter  $P$ . For  $P$  slightly above 1, the amplitude of oscillations  $A \approx P-1$  and the frequency is  $\Omega \approx P^{-1/2}$ . So, in qualitative agreement with the experiment, near the threshold the amplitude increases approximately linearly with  $P$ , and the frequency slowly decreases with  $P$ .

While the model Eq.(1) explains the nature of the layer oscillations, it does not address the mechanism of the instability which leads to the oscillations. Indeed, since there is always some dissipation due to friction and inelastic particle collisions, the oscillations would decay, and the stable equilibrium bed thickness at which the drag force balances gravity, would be reached. To overcome dissipation, an additional instability mechanism is needed to excite the layer oscillations. The mechanism of this instability is related to the known mechanism of instability for deep fluidized beds [12], in which it is caused by the inertia of particles in the gas flow and leads to the time delay between the volume fraction variations and the drag force changes. Similarly, we can assume that the drag force  $\Gamma$  is not enslaved to the thickness the

layer  $h$ , but approaches  $\gamma/h$  asymptotically. This additional degree of freedom can be described by the equation  $\alpha\Gamma_t = \gamma h^{-1} - \Gamma$ , where parameter  $\alpha$  controls the rate of inertia in the dependence between  $\Gamma$  and  $h$ . We shall also modify the equation for the layer thickness dynamics (1) to include a thickness-dependent dissipation. Indeed, the amount of dissipation varies strongly as a function of the layer thickness, as it affects the frequency of inelastic collision among grains. As the thickness approaches the close-packed limit, the number of collisions, and the dissipation rate, diverge. We assume that this effect is captured by an additional dissipative term  $-\sigma h_t/(h - h_0)^2$  (the actual power of singularity at  $h = h_0$  is not important here). Now, the extended model in non-dimensional form reads

$$H_{TT} = F - 1 - \frac{\sigma' H_T}{(H - 1)^2}, \quad (3)$$

$$\alpha' F_T = \frac{P}{H} - F, \quad (4)$$

where  $F = \Gamma/g\rho$ ,  $\alpha' = \alpha(g/h_0)^{1/2}$ ,  $\sigma' = \sigma(gh_0^3)^{-1/2}$ . Additional relaxation dynamics described by Eq.(4) directly leads to an instability of the thin fluidized layer. Linearizing Eqs.(3),(4) near the fixed point  $F = 1$ ,  $H = P$  yields the dispersion equation for perturbations  $\propto \exp(-i\Omega T)$ ,

$$(1 - i\alpha\Omega) \left[ \Omega^2 + \frac{i\sigma\Omega}{(P - 1)^2} \right] = \frac{1}{P}, \quad (5)$$

where we dropped primes at the non-dimensional parameters  $\alpha$  and  $\sigma$ . At small  $\alpha$  and  $\sigma$ , the complex frequency of layer oscillations is given by

$$\Omega \approx P^{-1/2} + \frac{i}{2} \left[ \frac{\alpha}{P} - \frac{\sigma}{(P - 1)^2} \right]. \quad (6)$$

As one can see from this formula, the instability always occurs at large enough  $P$ . Notice that for small  $\alpha$  and  $\sigma$ , the solution of Eqs.(3),(4) at large  $T$  approaches that of Eq.(2) with initial conditions  $H(0) = 1$ ;  $H_T(0) = 0$ . This is not surprising, since these conditions are enforced by diverging dissipation rate at  $H = 1$ , and during the rest of the oscillation cycle, non-conservative corrections are negligibly small.

To conclude, in this paper we studied the dynamics of a shallow fluidized granular layer. Experiments with air-driven shallow fluidized bed showed that above fluidization threshold, the layer exhibits oscillations at a certain frequency. These oscillations are in fact propagating waves which have a structure of small disordered spirals. At larger airflow speeds, in addition to the high-frequency spiral waves, low-frequency short-wavelength perturbations are observed in the bed. It is feasible that these small “bubbles” are formed via subharmonic excitation by the primary high-frequency oscillations, as in the Faraday instability. We proposed a simple dynamical model describing high-frequency oscillations in which

the layer is driven by the airflow drag force and gravity. The drag force in turn depends on the volume fraction of particles in the layer, and therefore on the height of the layer surface. The underlying assumptions for this model are based on experimental facts and the intuitive physical picture, and a systematic derivation of the model from the first principles may yield more complicated relations among the layer parameters. Still, this model describes the instability leading to the layer oscillations, and agrees on a qualitative level with the observed dependence of the oscillation magnitude and frequency on the airflow rate. A more detailed study of the model including its systematic derivation and generalization towards spatiotemporal dynamics will be the subject of a separate publication.

Authors are grateful to A.Didwania,T.Shinbrot, and H.Swinney for useful discussions. This research was supported by the Energy Research Program of the Office of Basic Energy Sciences at the US Department of Energy (grants # DE-FG03-95ER14516 and DE-FG03-96ER14592).

- 
- [1] H. M. Jaeger, S.R. Nagel and R. P. Behringer, Physics Today, **49**, 32 (1996); Rev. Mod. Phys. **68**, 1259 (1996).
  - [2] P. Umbanhowar, F. Melo and H.L. Swinney, Nature **382**, 793 (1996).
  - [3] T.Shinbrot, A.Alexander, F.J.Muzzio, Nature, **397**, 675 (1999).
  - [4] J.F.Davidson and D.Harrison, *Fluidized Particles*, Cambridge Univ. Press, London, 1963.
  - [5] A.M.Squires, M. Kwaik, and A.A.Avidan, Science, **230**, 1329 (1985).
  - [6] L.S.Tsimring, R.Ramaswamy, and P.Sherman, Phys. Rev. E, **60**, 7126 (1999).
  - [7] A.Kudrolli and J.P.Gollub, Physica D, **97**, 133 (1996).
  - [8] A similar filtering technique has been employed by A.La Porta and C.M.Surko [Physica D, **123**, 21 (1998)], and A.L.Lin et al. Phys. Rev. Letters, **84**, 4242 (2000).
  - [9] MPEG movie created from these images is located at <http://inls.ucsd.edu/grain/fluidbed>.
  - [10] H.Chate and P.Manneville, Physica A, **224**, 348 (1996).
  - [11] Q.Ouyang, and J.-M.Flesselles, Nature, **379**, 143 (1996).
  - [12] G.K.Batchelor, J.Fluid Mech., **193**, 75 (1988).